Boundary condition and initial value effects in the reaction–diffusion model of interface trap generation/recovery*

Luo Yong(罗勇)[1], Huang Daming(黄大鸣)[1,†], Liu Wenjun(刘文军)[1], and Li Mingfu(李名复)[1,2]

(1 State Key Laboratory of ASIC & System, Department of Microelectronics, Fudan University, Shanghai 201203, China)

(2 SNDL, ECE Department, National University of Singapore, Singapore 117576, Singapore)

Abstract: A simple standard reaction–diffusion (RD) model assumes an infinite oxide thickness and a zero initial interface trap density, which is not the case in real MOS devices. In this paper, we numerically solve the RD model by taking into account the finite oxide thickness and an initial trap density. The results show that trap generation/passivation as a function of stress/recovery time is strongly affected by the condition of the gate-oxide/poly-Si boundary. When an absorbent boundary is considered, the RD model is more consistent with the measured interface-trap data from CMOS devices under bias temperature stress. The results also show that non-negligible initial traps should affect the power index n when a power law of the trap generation with the stress time, t^n, is observed in the diffusion limited region of the RD model.

Key words: reaction–diffusion model; interface-trap generation/passivation; negative bias temperature instability; charge pumping; direct-current current–voltage

DOI: 10.1088/1674-4926/30/7/074008 **PACC:** 7340Q **EEACC:** 2560B

1. Introduction

The negative bias temperature instability (NBTI) is one of the most critical reliability concerns for present CMOS technology[1,2]. It is widely believed that NBTI originates from the generation/passivation of interface traps[3] and/or the trapping/detrapping of oxide-charge[4]. By far the most quoted model for the generation/passivation of interface traps is the reaction–diffusion (RD) model[5–14]. The simple standard RD model assumes an infinitely thick oxide layer, a zero initial interface trap density, and purely diffusive transport of hydrogen particles[5–10]. In the diffusion limited region, the model can be solved analytically and predicts a power law dependence (t^n) of the interface-trap generation on the stress time t. The power index n is 1/6 for the diffusion of H_2 and 1/4 for that of H. The model also predicts a relative recovery of near 50% after the stress has been stopped for the same period as the stress time. It further predicts that both, n and the relative recovery, are temperature independent. While the qualitative properties of interface-trap generation and recovery are predicted by the standard RD model, quantitative deviations are often observed when the model is compared with experimental data. To some extend the standard model to more useful for practical situations, the RD model with a finite oxide thickness was solved analytically more than ten years ago[11]. Using the Laplace transform, Ogawa *et al.*[11]solved the RD model for a finite oxide thickness with an absorbent boundary at a SiO_2/poly-Si interface. However, Ogawa's analytical method can only give the results for the stress phase not the recovery phase, and thus no comparison with recent NBTI observations is possible[11]. Recently, the boundary condition at the oxide/poly-Si interface was considered[12] to account for the observed saturation of the interface-trap generation at long stress times. In contrast to the infinite oxide thickness, a model with a very thin oxide layer and a thick poly-Si layer is applied[13,14] to account for the observed quick recovery of the interface-trap generation at short (~1 s) times after the stress is stopped. More recently, to account for the temperature dispersion of n, the RD model has been extended to the case of defect-controlled transport and the appropriate boundary and initial conditions are also discussed[15–17]. However, only the effect of the Si/SiO_2 interface is considered in Ref. [16]. The interface of SiO_2/poly-Si is not taken into account, i.e., an infinite oxide thickness is assumed. Further, only the stress is considered, not the recovery phase.

The physical quantity commonly measured in a NBTI investigation is the threshold voltage shift ΔV_{TH}. Since the realization of the importance of both, interface-traps and oxide-charge, and the recovery effect to NBTI[18–20], some data have been reported on both stress and recovery phases using interface-trap measurement methods, such as charge pumping (CP)[4,21–23] and direct-current current–voltage (DCIV)[22,24] techniques. These data can be used to test the RD model. It has been observed that the experimental data are mostly not consistent with the standard RD model. The measured power index n in the stress phase often deviates from 1/6. The relative recovery is mostly less than 50% and is temperature dependent. In addition, a permanent interface-trap component may be present in the recovery phase[25]. Therefore, to better understand interface-trap generation/passivation in NBTI, it

* Project supported by the Micro/Nanoelectronics Science & Technology Innovation Platform, Fudan University.

† Corresponding author. Email: dmhuang@fudan.edu.cn

Received 5 December 2008, revised manuscript received 20 February 2009

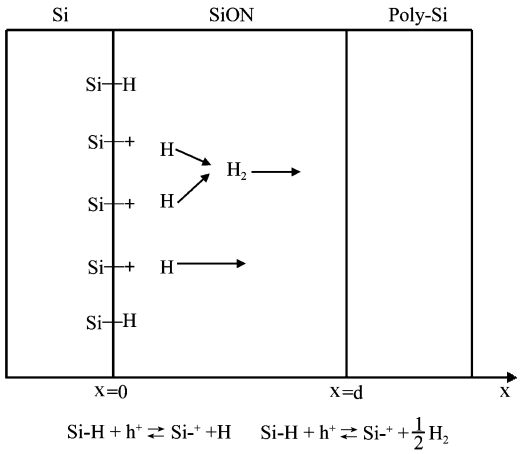

Fig. 1. Schematic diagram showing the reaction–diffusion model, which describes the generation of interface traps at the Si/SiON interface.

is necessary to reassess the RD model using a more practical structure and conditions to see if the model is consistent with the experimental results. In this paper, we solve the RD model numerically by taking into account the effects of a finite oxide thickness and initial interface traps. In contrast to all of the previous calculations, we solve the RD model in both the stress and recovery phases by considering a finite oxide thickness with reflective and absorbent boundary conditions at the SiO_2/poly-Si interface, so that the theoretical calculations and experimental observations of NBTI can be compared more reasonably and quantitatively. A smaller interface-trap recovery $\Delta N_{IT}(t)$ and a permanent component are predicted when the boundary is absorbent. We show that the RD model is more consistent with experimental results if the proper boundary and initial conditions are considered.

2. Standard reaction–diffusion model

The RD model states that when a pMOSFET is biased into inversion, the Si–H bonds at the Si/oxide interface capture holes in the channel and dissociate into positively charged interface traps and hydrogen particles. The latter diffuse away either in the form of atomic H or molecular H_2[5–10] (see Fig. 1).

Earlier experiments showed that the power index n of NBTI is close to 0.25, in accordance with the RD model's prediction of the H diffusion. However, recent experimental results show that the earlier experiments are not directly comparable with the RD model due to the recovery effect, and a more reliable power index of 0.17 is obtained by the improved experimental methods[9]. Therefore, H_2 diffusion is more likely in the NBTI process[9] and only H_2 diffusion is discussed in this paper. In this case, the process can be described by Eqs. (1)–(6).

$$\frac{dN_{IT}(t)}{dt} = k_F(N_0 - N_{IT}(t)) - k_R\sqrt{N_{H_2}(0,t)}N_{IT}(t), \quad (1)$$

$$N_{IT}(t)|_{t=0} = N_{IT0}, \quad (2)$$

$$\frac{dN_{H_2}}{dt} = D_{H_2}\nabla^2 N_{H_2}, \qquad 0 < x < d, \quad (3)$$

$$-D_{H_2}\frac{\partial N_{H_2}(x,t)}{\partial t}|_{x=0} = \frac{dN_{IT}(t)}{dt}, \quad (4)$$

$$-D_{H_2}\frac{\partial N_{H_2}(x,t)}{\partial t}|_{x=d} = k_p N_{H_2}(x,t)|_{x=d}, \quad (5)$$

$$N_{H_2}(x,t)|_{t=0} = N_{H_2}(x,0), \quad (6)$$

where $N_{IT}(t)$ is the density of interface traps, N_0 is the density of Si–H bonds, $k_F(k_R)$ is the forward (reverse) reaction constant, $N_{H_2}(x,t)$ is the concentration of H_2 in the oxide, D_{H_2} is the diffusion coefficient, and k_p is the annihilation rate of H_2 at the boundary $x = d$. The standard RD model assumes that (1) the oxide thickness d is infinite and (2) both N_{IT0} and $N_{H_2}(x,0)$ are 0 for a fresh device. Under these assumptions, the boundary condition Eq. (5) can be replaced by the conservation law, which can be written approximately as

$$N_{IT} = 2\int_0^\infty N_{H_2}(x,t)dt \approx pN_{H_2}(0,t)\sqrt{D_{H_2}t}, \quad (7)$$

where $p \approx 3$ is a dimensionless constant[9]. Based on the above assumptions, one can obtain an analytical solution for $N_{IT}(t)$ in the diffusion limited region,

$$N_{IT}(t) = \left(\frac{\sqrt{p}k_F N_0}{k_R}\right)^{2/3}(D_{H_2}t)^{1/6}. \quad (8)$$

Figure 2(a) shows numerical solutions of the standard RD model for H_2 diffusion, in both the stress and the recovery phases plotted on a linear scale. In Fig. 2(b), the same result for the stress phase is plotted on a log–log scale. The most important characteristic predicted by the standard RD model for H_2 diffusion is that interface-trap generation under a stress follows a power law, $N_{IT}(t) \sim t^n$ with $n = 1/6$ in the diffusion limited region. The relative recovery is ~50% when the recovery time is equal to the stress time. Both the $t^{1/6}$ dependence and relative recovery (~50%) are temperature independent. Figure 2(c) plots the $N_{H_2}(x)$ profiles for a few times in the stress phase. As shown, $N_{H_2}(x)$ can be well approximated by triangles with diffusion fronts at $\sim 3\sqrt{D_{H_2}t}$ (but not $\sqrt{D_{H_2}t}$).

3. RD model with absorbent or reflective boundary

When the oxide thickness is finite, the boundary condition of Eq. (5) should be considered. Since the detailed properties of the oxide/poly-Si interface are not understood, we model the boundary by two typical cases, i.e., the absorbent or reflective conditions. In the case of an absorbent boundary, $k_p = \infty$ and Equation (5) is replaced by

$$N_{H_2}(x,t)\big|_{x=d} = 0. \quad (9)$$

For a reflective boundary, $k_p = 0$ and Equation (5) is replaced by

$$\left.\frac{\partial N_{H_2}(x,t)}{\partial x}\right|_{x=d} = 0. \quad (10)$$

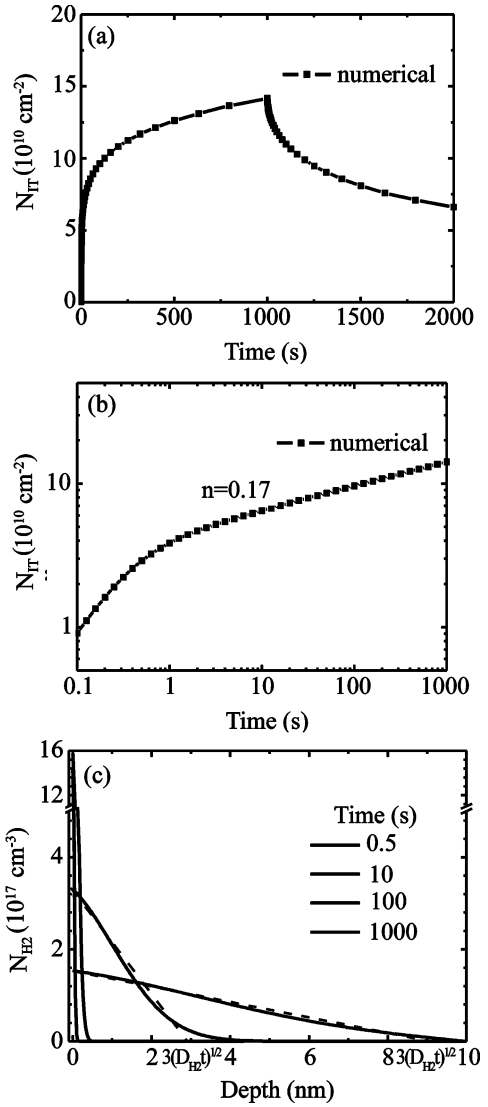

Fig. 2. Numerical solution of the standard RD model for H_2 diffusion. The parameters used in the calculation are $N_0 = 1.0 \times 10^{14}$ cm^{-2}, $k_F = 1 \times 10^{-3}$ s^{-1}, $k_R = 1.8 \times 10^{-9}$ cm^3/s, and $D_{H_2} = 1 \times 10^{-16}$ cm^2/s. (a) Time evolution of interface-traps $N_{IT}(t)$ plotted on a linear scale. (b) The same data for the stress phase of Fig. 1(a), plotted on a log–log scale. (c) Hydrogen profiles $N_{H_2}(x, t)$ at several times in the stress phase. In the diffusion-limited region, $N_{H_2}(x, t)$ can be well approximated by triangles with diffusion fronts at $\sim 3\sqrt{D_H t}$, as shown by dashed lines.

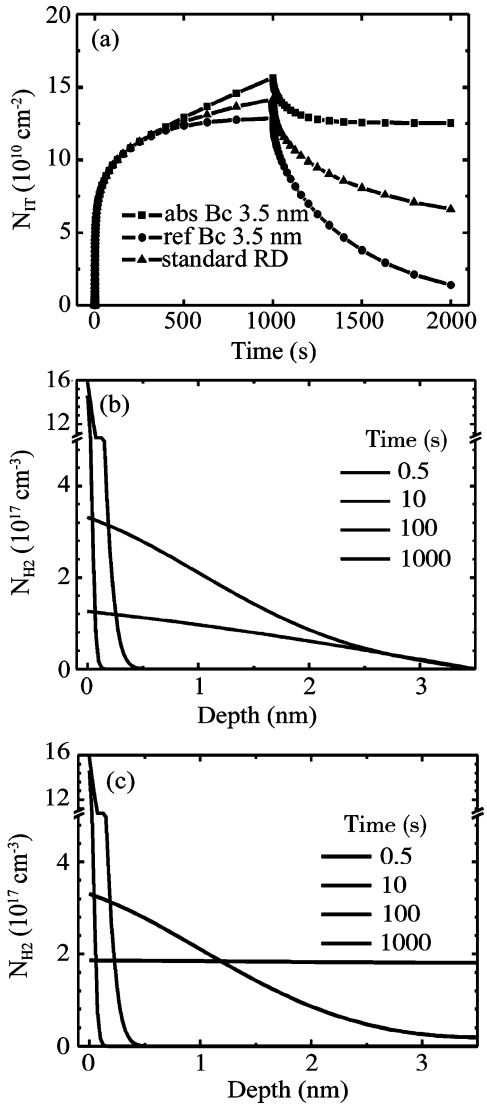

Fig. 3. (a) Numerical solution of the standard RD model and of that with an absorbent or reflective boundary conditions for a finite oxide thickness. Evolution of the H_2 profile (b) with an absorbent boundary and (c) with a reflective boundary at a few time intervals in the stress phase.

The RD model of Eqs. (1)–(6) with an absorbent ($k_p = \infty$) or reflective ($k_p = 0$) boundary and with zero initial conditions [$N_{IT0} = 0$, $N_{H0}(x) = 0$] is numerically solved. The results for $N_{IT}(t)$ are presented in Fig. 3(a). In both cases, d (= 3.5 nm) and the other parameters are kept constant. Figure 3(a) also presents the result of the standard RD model for a thick oxide layer. As shown, for a short stress time t (< 100 s) when $3\sqrt{D_H t} < d$, the boundary effect is negligible. For large t (> 300 s) and $3\sqrt{D_H t} > d$, the boundary effect is not negligible and becomes very important in the recovery phase ($t >$ 1000 s). Compared to the standard RD model, $N_{IT}(t)$ in the stress phase for large t increases more rapidly for the absorbent boundary and less rapidly for the reflective boundary. In the recovery phase, the fractional recovery at t = 2000 s a with respect to $N_{IT}(t = 1000$ s) is less than 50% for the absorbent boundary. In particular, the recovery quickly saturates and a permanent-like (unrecoverable) component shows up. For the reflective boundary, in contrast, the fractional recovery is larger than 50% and no permanent component is expected.

The above results are easily understood with the help of the $N_{H_2}(x, t)$ profiles plotted in Figs. 3(b) and 3(c) for an absorbent and reflective boundary, respectively. At the beginning of the stress phase, N_{IT}(t) and $N_{H_2}(x, t)$ follow the standard RD model. For large t, when the diffusion front reaches the $x = d$ boundary, N_{IT}(t) is affected by the boundary. Under absorbent conditions, the H_2 particles are all lost at the boundary, which enhances the generation of N_{IT}(t) in the stress phase and leads to a permanent N_{IT}(t) component in the recovery phase. Under reflective conditions, the H_2 particles reaching the boundary are totally reflected, which suppresses the generation of interface traps in the stress phase and accelerates the recovery in the recovery phase.

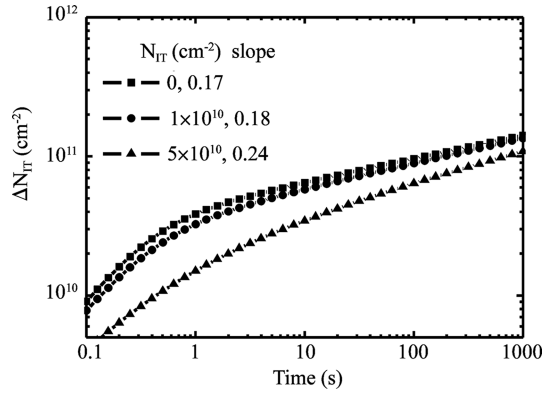

Fig. 4. Numerical solution $\Delta N_{IT}(t)$ from the RD model with three different N_{IT0}.

4. RD model with non-zero initial value

During the CMOS manufacturing process, hydrogen is used to passivate Si dangling bonds. Some of the dangling bonds which are not passivated by H form interface traps N_{IT0} in fresh devices. The presence of N_{IT0} may be observed by experiment methods, such as charge pumping.

When N_{IT0} is not zero, the rate equation (1) should be rewritten as

$$\frac{\mathrm{d}\Delta N_{IT}(t)}{\mathrm{d}t} = k_F[N_0 - \Delta N_{IT}(t)] - k_R\sqrt{N_{H_2}(0,t)}\Delta N_{IT}(t)$$

$$-\left[k_F + k_R\sqrt{N_{H_2}(0,t)}\right]N_{IT0}, \qquad (11)$$

where $\Delta N_{IT}(t) = N_{IT}(t) - N_{IT0}$ are the generated interface traps under stress. Compared to Eq. (1) for $N_{IT}(t)$, the generation rate $\mathrm{d}N_{IT}(t)/\mathrm{d}t$ reduces with increasing N_{IT0} due to the last term $-(k_F + k_R\sqrt{N_{H_2}(0,t)})N_{IT0}$. This term is more pronounced for small t when N_{IT0} is comparable to or even larger than $N_{IT}(t)$. For large t when $N_{IT0} \ll N_{IT}(t)$, the effect of N_{IT0} is negligible.

Figure 4 presents numerical solutions of the RD model for $N_{IT}(t)$ with three different N_{IT0}, plotted on a log–log scale. To decouple the effects of the boundary and the initial value, an infinite thick oxide layer is assumed in this calculation. As Figure 4 shows, even when the initial value (1×10^{10} cm^{-2}) is one order of magnitude less than the generated $\Delta N_{IT}(t)$ at t = 1000 s ($\sim 1 \times 10^{11}$cm^{-2}), the effect of the initial value is not negligible. For $N_{IT0} = 5 \times 10^{10}$ cm^{-2}, which is about 1/2 that of $N_{IT}(t = 1000\ \mathrm{s})$, the effect is significant as the power index n increases from 0.17 to 0.24. Neglecting the initial value effect may lead to the misinterpretation of experimental results, for example, from H_2 to H diffusion.

5. Comparison with experimental results

The devices used in the investigation are p-MOSFETs fabricated with a poly-Si/SiON gate stack. SiON was grown by thermal oxidation followed by plasma nitridation and post-deposition thermal annealing. The oxide thickness is 3.5 nm. A CP method was used for the interface-trap measurements in the NBTI characterization. The density of interface traps $N_{IT}(t)$ is proportional to the measured CP current $I_{cp}(t)$[26] and is calculated from $I_{cp}(t)$ by considering the temperature dependence of I_{cp} for a fixed N_{IT}[27]. Figure 5(a) presents the measured $N_{IT}(t)$ for the devices in both the stress and the recovery phases at 25, 100, and 150 °C plotted in the same figure to show the temperature dependence. The most important feature observed in Fig. 5(a) is that the relative recoveries, defined as $R = -[N_{IT}(2000\ \mathrm{s}) - N_{IT}(1000\ \mathrm{s})]/[N_{IT}(1000\ \mathrm{s}) - N_{IT}(0\ \mathrm{s})]$, are all less than 50%. This is consistent with previously published CP results[4, 21–23]. Moreover, R decreases with increasing T (29% at 25 °C, 20% at 100 °C, and 14% at 150 °C).

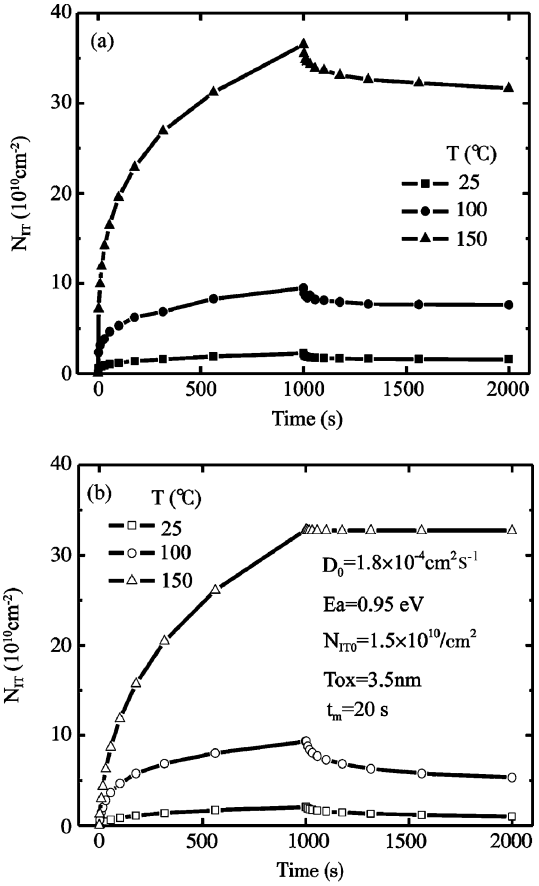

Fig. 5. (a) Interface-trap density $N_{IT}(t)$ measured by CP in the stress and recovery phases at T = 25, 100, 150 °C; (b) Numerical solution of the RD model with the absorbent boundary at T = 25, 100, 150 °C. The diffusion constant at different temperatures T is assumed to follow an Arrhenius-like behavior with $D_0 = 1.8 \times 10^{-4}$ cm^2/s and E_a = 0.95 eV.

As shown in Fig. 3(a), the above features are clearly not consistent with the standard RD model, which predicts R to be about 50% and to be temperature independent. The results are also not compatible with the RD model with a reflective boundary. For a reflective boundary in the recovery phase, the RD model predicts R to be larger than 50% and to increase with increasing temperature. R reaches near 100% at high T (for example, 150 °C), which is completely opposite to the experimental observations.

We show here that the experimental results are possibly

explained by the RD model with an absorbent boundary. To simulate the experimental results at different T, we solve the RD model using an absorbent boundary. The measurement delay has been considered in the calculation since its effect can be predicted by the RD model itself. According to the CP experiments, a delay time of 20 s is used. The diffusion coefficients are assumed to follow an Arrhenius law, while other constants, such as k_F and k_R, are assumed to be temperature independent for simplicity, as their T-dependences are very similar and will largely cancel out[15]. Figure 5(b) presents the numerical solutions of the RD model with an absorbent boundary for a d = 3.5 nm oxide at 25, 100, and 150 °C. By comparing Fig. 5(b) with Fig. 5(a), it is shown that the main features of the experimental results are well reproduced by the RD model. In the stress phase, the rapid increase in $N_{IT}(t)$ with T is due to the increase of the diffusion constant. In the recovery phase, R is smaller than 50% and decreases with increasing T due to the absorbent boundary. A permanent $N_{IT}(t)$ component is predicted due to the loss of H_2 in the boundary. This component is larger at higher T when more H_2 is lost due to the faster H_2 diffusion from the Si/oxide to the oxide/poly-Si interface.

We show that proper boundary and initial conditions improve the agreement of the RD model with the experiments. Since NBTI includes both interface and oxide traps, experimental results, even those like CP, may contain a contribution from oxide traps. Therefore, care should be taken to compare the RD model with experimental results from interface traps only and not from oxide traps.

6. Conclusions

The standard RD model for an infinitely thick oxide is not consistent with the interface-trap generation/passivation results measured by CP in the stress/recovery phase in NBTI experiments. By numerically solving the RD model with an oxide of finite thickness, the main features of the experimental results are reproduced by the RD model with appropriate boundary conditions. A smaller ($R < 50\%$) and T dependent recovery of the stress-induced interface-trap generation is experimentally observed and reproduced by the RD model with an absorbent boundary at the oxide/poly-Si interface. A permanent-like interface-trap component is also predicted by the model. In addition to the boundary condition, numerical calculation shows that the initial value of the interface traps may significantly affect the power index n derived from the RD model in the diffusion limited region.

References

[1] Schroder D K, Babcock J A. Negative bias temperature instability: road to cross in deep submicron silicon semiconductor manufacturing. J Appl Phys, 2003, 94: 1

[2] Reddy V, Krishnan A T, Marshall A, et al. Impact of negative bias temperature instability on digital circuit reliability. IEEE IRPS Tech Dig, 2002: 248

[3] Varghese D, Saha D, Mahapatra S, et al. On the dispersive versus Arrhenius temperature activation of NBTI time evolution in plasma nitrided gate oxides: measurements, theory, and implications. IEDM Tech Digest, 2005: 701

[4] Huard V, Denais M. Hole trapping effect on methodology for DC and AC negative bias temperature instability measurements in pMOS transistors. IEEE IRPS Tech Dig, 2004: 40

[5] Jeppson K O, Svensson C M. Negative bias stress of MOS devices at high electric fields and degradation of MNOS devices. J Appl Phys, 1977, 48: 2004

[6] Alam M A. A critical examination of the mechanics of dynamic NBTI for p-MOSFETs. IEDM Tech Dig, 2003: 345

[7] Alam M A, Mahapatra S. A comprehensive model of PMOS NBTI degradation. Microelectron Reliab, 2005, 45: 71

[8] Yang J B, Chen J P. Analytical reaction-diffusion model and the modeling of nitrogen-enhanced negative bias temperature instability. Appl Phys Lett, 2006, 88: 172109

[9] Krishnan A T, Chakravarthi S, Nicollian P, et al. Negative bias temperature instability mechanism: the role of molecular hydrogen. Appl Phys Lett, 2006, 88: 153518

[10] Kumar S V, Kim C H, Sapatnekar S S. An analytical model for negative bias temperature instability. ICCAD, 2006: 493

[11] Ogawa S, Shiono N. Generalized diffusion-reaction model for the low-field charge build up instability at the Si–SiO_2 interface. Phys Rev B, 1995, 51: 4218

[12] Aono H, Murakami E, Okuyama K, et al. Modeling of NBTI degradation and its impact on electric field dependence of the lifetime. IEEE IRPS Tech Dig, 2004: 23

[13] Chakravarthi S, Krishnan S, Reddy V, et al. A comprehensive framework for predictive modeling of negative bias temperature instability. IEEE IRPS Tech Dig, 2004: 273

[14] Krishnan A, Chancellor C, Chakravarthi S, et al. Material dependence of hydrogen diffusion: implications for NBTI degradation. IEDM Tech Dig, 2005: 341

[15] Kaczer B, Arkhipov A, Degraeve R, et al. Disorder-controlled-kinetics model for negative bias temperature instability and its experimental verification. IEEE IRPS Tech Dig, 2005: 381

[16] Grasser T, Gos W, Kaczer B. Dispersive transport and negative bias temperature instability: boundary conditions, initial conditions, and transport models. IEEE Trans Devices Mater Reliab, 2008, 8: 79

[17] Grasser T, Selberherr S. Modeling of negative bias temperature instability. Journal of Telecommunications and Information Technology, 2007, 92: 102

[18] Chen G, Li M F, Ang C H, et al. Dynamic NBTI of p-MOS transistors and its impact on MOSFET scaling. IEEE Electron Device Lett, 2002, 23: 734

[19] Tsujikawa S, Mine T, Watanabe K, et al. Negative bias temperature instability of pMOSFETs with ultra-thin SiON gate dielectrics. IRPS Tech Dig, 2003: 183

[20] Ershov M, Saxena S, Karbasi H, et al. Dynamic recovery of NBTI in p-type MOSFETs. Appl Phys Lett, 2003, 83: 1647

[21] Huard V, Denais M, Parthasarathy C. NBTI degradation: from physical mechanisms to modeling. Microelectron Reliab, 2006, 46: 1

[22] Yang T, Li M F, Shen C, et al. Fast and slow dynamic NBTI components in p-MOSFET with SiON dielectric and their impact on device life-time and circuit application. VLSI Tech Dig, 2005: 92

[23] Mahapatra S, Ahmed K, Varghese D, et al. On the physical mechanism of NBTI in silicon oxynitride p-MOSFETs: can differences in insulator processing conditions resolve the interface trap generation versus hole trapping controversy? IRPS Tech Dig, 2007: 1

[24] Neugroschel A, Ersuker G, Choi R. Applications of DCIV method to NBTI characterization. Microelectron Reliab, 2007, 47: 1366

[25] Grasser T, Kaczer B, Hehenberger P, et al. Simultaneous extraction of recoverable and permanent components contributing to bias-temperature instability. IEDM Tech Dig, 2007: 801

[26] Groeseneken G, Maes H E, Beltran N, et al. A reliable approach to charge-pumping measurements in MOS transistors. IEEE Trans Electron Devices, 1984, 31: 42

[27] Van den Bosch G, Groeseneken G , Heremans P, et al. Spectroscopic charge pumping: a new procedure for measuring interface trap distributions on MOS Transistors. IEEE Trans Electron Devices, 1991, 38: 1820